Cyclic AMP compartmentation due to increased cAMP-phosphodiesterase activity in transgenic mice with a cardiac-directed expression of the human adenylyl cyclase type 8 (AC8)

Marie Georget, Philippe Mateo, Grégoire Vandecasteele, Larissa Lipskaia, Nicole Defer, Jacques Hanoune, Jacqueline Hoerter, Claire Lugnier, Rodolphe Fischmeister

Cyclic AMP compartmentation due to increased cAMP-phosphodiesterase activity in transgenic mice with a cardiac-directed expression of the human adenylyl cyclase type 8 (AC8)

Marie Georget, Philippe Mateo, Grégoire Vandecasteele, Larissa Lipskaia[*], Nicole Defer[*], Jacques Hanoune[*], Jacqueline Hoerter, Claire Lugnier[£] and Rodolphe Fischmeister[$]

Laboratoire de Cardiologie Cellulaire et Moléculaire, INSERM U-446, Université Paris-Sud, Faculté de Pharmacie, F-92296 Châtenay-Malabry, France

[*]Laboratoire de Régulation des Gènes et Signalisation Cellulaire, INSERM U-99, Hôpital Henri-Mondor, F-94010 Créteil, France

[£]Laboratoire de Pharmacologie et de Physico-Chimie des Interactions Cellulaires et Moleculaires, CNRS-UMR 7034, Université Louis Pasteur de Strasbourg, Faculté de Pharmacie, F-67401, Illkirch, France

[$]Corresponding author: Rodolphe Fischmeister, INSERM U-446, Université Paris-Sud, Faculté de Pharmacie, 5, Rue J.-B. Clément, F-92296 Châtenay-Malabry Cedex, France. Tel.: 33-1-46 83 57 71. Fax: 33-1-46 83 54 75

E-mail: Fisch@vjf.inserm.fr

ABSTRACT

Hearts from AC8TG mice develop a higher contractility (LVSP) and larger Ca^{2+} transients than NTG mice, with surprisingly no modification in L-type Ca^{2+} channel current ($I_{Ca,L}$)(1). In this study, we examined the cardiac response of AC8TG mice to ß-adrenergic and muscarinic agonists and IBMX, a cyclic nucleotide phosphodiesterase (PDE) inhibitor. Stimulation of LVSP and $I_{Ca,L}$ by isoprenaline (ISO, 100 nM) was 2-fold smaller in AC8TG *vs.* NTG mice. In contrast, IBMX (100 µM) produced a 2-fold higher stimulation of $I_{Ca,L}$ in AC8TG *vs.* NTG mice. IBMX (10 µM) increased LVSP by 40% in both types of mice, but contraction and relaxation were hastened in AC8TG mice only. Carbachol (10 µM) had no effect on basal contractility in NTG hearts but decreased LVSP by 50% in AC8TG mice. PDE assays demonstrated an increase in cAMP-PDE activity in AC8TG hearts, mainly due to an increase in the hydrolytic activity of PDE4 and PDE1 toward cAMP and a decrease in the activity of PDE1 and PDE2 toward cGMP. We conclude that cardiac-expression of AC8 is accompanied by a rearrangement of PDE isoforms, leading to a strong compartmentation of the cAMP signal which shields L-type Ca^{2+} channels and protects the cardiomyocytes from Ca^{2+} overload.

Key Words: transgenic mouse ● adenylyl cyclase ● cAMP ● isolated heart ● L-type Ca^{2+} current ● ß-adrenoceptors ● muscarinic receptors ● phosphodiesterase-compartmentation.

INTRODUCTION

Cyclic AMP is one of the major second messengers involved in the regulation of cardiac function. Its production is controlled by the activity of adenylyl cyclase (AC), which is enhanced via heterotrimeric Gs protein, like during activation of β-adrenoceptors by catecholamines. A rise in intracellular cAMP leads to activation of cAMP-dependent protein kinase (PKA) which phosphorylates a multitude of regulatory proteins controlling the force of contraction and its relaxation: these include the L-type Ca^{2+} channel, phospholamban, myofilament proteins and ryanodine receptors (2). In contrast to catecholamines, acetylcholine (ACh) released during activation of the parasympathetic system generates a negative chronotropic and inotropic effect on the heart. By acting on M_2-muscarinic receptors, ACh opposes the action of the sympathetic system mainly through G_i protein inhibition of AC (3,4).

Cyclic AMP production by adenylyl cyclase is counterbalanced by its hydrolysis into 5'-AMP by cyclic nucleotide phosphodiesterases (PDE, 5-7). PDEs constitute a large multigenic family out of which four members have been found and characterized in the heart: PDE1, which is activated by Ca^{2+}/calmodulin (CaM); PDE2, which is stimulated by cGMP; PDE3, which is inhibited by cGMP; and PDE4, which is insensitive to cGMP. While PDE3 and PDE4 hydrolyze cAMP, PDE1 hydrolyzes equally cAMP and cGMP and PDE2 hydrolyzes both with a lower apparent K_m for cGMP than for cAMP (6-8).

Today, it has become well established that an increase in intracellular cAMP level may lead to different effects on cardiac function, depending on the pathway used. For instance, activation of prostaglandin E1 (PGE_1), glucagon-like peptide-1 (GLP-1) and ß-adrenergic receptors, which all increase cAMP level, produce different effects on cardiac function (9-12): PGE_1

does not modify contractile activity, while GLP-1 and isoprenaline, a ß-adrenergic agonist, exert negative and positive effects on myocyte contraction, respectively (11, 12). Functional and/or physical compartmentation of cAMP may provide a means by which a cell discriminates among different external stimuli acting on a promiscuous second messenger cascade (13, 14). A typical example of such compartmentation is given by the distinct effects on rat ventricular myocytes of $ß_1$- and $ß_2$-adrenergic receptor (AR) agonists. While both ß-AR agonists increase cAMP concentration, L-type Ca^{2+} channel current ($I_{Ca,L}$) and contraction, only $ß_1$-AR agonists induce the phosphorylation of phospholamban and contractile proteins, leading to an additional lusitropic effect not observed with $ß_2$-AR agonists (15, 16). The cAMP signal generated by $ß_2$-AR pathway has been shown to be highly localized to the sarcolemma (17, 18) possibly through a G_i protein-dependent mechanism (17, 18).

In a recent study, we proposed that compartmentation of cAMP might also serve a protective role in preserving cardiac myocytes from a deleterious Ca^{2+} overload (1). Using the transgenic mouse line AC8TG, in which the human neuronal Ca^{2+}/calmodulin activated AC8 (19-21) protein is specifically expressed in cardiac myocytes by coupling the exogenous gene cDNA to the αMHC promoter (19-21), we found that the L-type Ca^{2+} channel current ($I_{Ca,L}$) was not enhanced in AC8TG mice, although these mice had a 2-fold increased cardiac function (1) as a result of a 7- and 4-fold increase in total AC and PKA activities, respectively (19-21). Since these mice showed no sign of hypertrophy or cardiomyopathy but on the contrary displayed all the hallmarks of an improved sarcoplasmic reticulum (SR) function (faster whole-heart and single-cell contractile relaxation, larger and shorter Ca^{2+} transients), we speculated that the additional cAMP production due to AC8 expression served to specifically activate Ca^{2+} uptake into the SR but not Ca^{2+} influx at the sarcolemma (1). In the present study, our aim was to give some clues on what might be the mechanisms responsible for the cAMP compartmentation that shields Ca^{2+} channels. We first examined how cardiac expression of

AC8 affected the β-adrenergic and muscarinic control of cardiac function and $I_{Ca,L}$. Next, we examined whether PDEs might play a role in this compartmentation, first by testing the effect of PDE inhibition on contractile activity and $I_{Ca,L}$ amplitude in non transgenic (NTG) and AC8TG mice, and second by measuring the activity of each PDE isoform in these two animal models.

MATERIALS AND METHODS

The investigation conforms with our institution guidelines defined by the European Community guiding principles in the care and use of animals and the French decree n°87/848 of October 19, 1987. Authorizations to perform animal experiments according to this decree were obtained from the French Ministère de l'Agriculture, de la Pêche et de l'Alimentation (n°7475, May 27, 1997).

Ex vivo physiology

Four to 5-months old mice were anaesthetized by intraperitoneal injection of pentothal (150 mg/kg). The heart was quickly removed, placed in oxygenated Krebs-Henseleit solution (95% O2 and 5% CO2, pH 7.35) containing low Ca^{2+} concentration (0.4 mM) and heparin. The aorta was cannulated on a 20-gauge cannula and perfused by the Langendorff method with a Krebs-Henseleit solution at constant pressure (75 mmHg). A small home made latex balloon was inserted in the left ventricle (LV) chamber. The temperature was monitored on line and maintained at 37±0.2°C throughout the experiments. All hearts were initially perfused with oxygenated Krebs-Henseleit solution at a perfusate Ca^{2+} concentration ($[Ca^{2+}]_o$) of 1.8 mM and the LV balloon was progressively inflated to isovolumic condition of work corresponding to an end diastolic pressure (EDP) of 5-8 mmHg. The water-filled balloon was connected to a pressure transducer (Statham gauge Ohmeda, Bilthoven, Holland) for continuous measurement of LV Systolic Pressure (LVSP) on a paper recorder (Astro-Med, West Warrick, UK). Contractile parameters were measured on-line by programming a PC-compatible 486/50 microcomputer in Assembly language (Borland) to determine heart rate (HR), LVSP, Rate-Pressure Product (RPP = LVSPxHR, used as an index of contractility), EDP and the following kinetic parameters: time to peak of contraction (t_{tp}), time for half relaxation ($t_{R1/2}$), and the

maximal values of the first derivatives of LVSP (+dLVSP/dt and -dLVSP/dt). To dissociate the specific changes in the kinetics of contraction and relaxation from those resulting from a modification of LVSP, these first derivatives were also expressed relative to LVSP (+dLVSP/dt/LSVP and -dLVSP/dt/LSVP). Some experiments were done under pacing conditions at a reduced $[Ca^{2+}]_o$ (1 mM). In this case, the hearts were stimulated at 680 bpm via platinum wires (stimulator HSE, Hugo Sachs Electronics, March-Hugstetten, Germany). Ten minutes of equilibration in isovolumic working conditions were imposed before beginning the experiment.

Preparation of mouse ventricular myocytes

Ventricular myocytes were isolated from the hearts of NTG and AC8TG mice as previously described (22). Three to 4-month old animals were anaesthetized by intraperitoneal injection of penthotal (150 mg/kg), the heart was quickly removed and placed into a cold Ca^{2+}-free Tyrode's solution. The aorta was cannulated and the heart was perfused with an oxygenated Ca^{2+}-free Tyrode's solution during 3-5 min using retrograde Langendorff perfusion, at 37°C. For enzymatic dissociation, the heart was perfused with Ca^{2+}-free Tyrode's solution containing collagenase D and protease XXIV during 10 minutes. Then, the heart was removed and placed into a dish containing an oxygenated Tyrode's solution supplemented with 0.2 mM Ca^{2+} at room temperature. The ventricles were separated from atria, cut in small pieces and triturated with a pipette to disaggregate myocytes. Ventricular cells were filtered on gauze and allowed to sediment by gravity during 10 min. The supernatant was removed and cells were suspended in 0.5 mM Ca^{2+}-Tyrode's solution. The procedure was repeated once again and at the end the cells were suspended in 1 mM Ca^{2+}-Tyrode's solution. The cells were stored at room temperature until use.

L-type Ca^{2+} channel current measurement

The whole-cell configuration of the patch-clamp technique was used to record L-type Ca^{2+} channel current ($I_{Ca,L}$). For routine $I_{Ca,L}$ measurements, the cells were depolarized every 8 s from a holding potential of -50 mV to 0 mV for 400 ms. At this holding potential, fast Na^+ current and T-type Ca^{2+} current were inactivated. External and internal (pipette) solutions contained Cs^+ instead of K^+ to eliminate K^+ currents. The electrical resistance of the patch pipette varied between 0.5 and 1.2 mΩ. All experiments were done at room temperature. A challenger VM (Kinetic, Atlanta, USA) generated voltage clamp protocols. The currents were measured by a patch-clamp amplifier (Biologic RK 400, Claix, France), filtered at 3 kHz and sampled at a frequency of 10 kHz. The maximal amplitude of $I_{Ca,L}$ was measured as the difference between the peak inward current at 0 mV and the current at the end of 400 ms pulse. Currents were not compensated for capacitive and leak currents. Two mV and 10 ms depolarizations from the holding potential were used to elicit capacitive currents, which were filtered at 10 kHz and sampled at a frequency of 20 kHz. Exponential analysis of these currents led to the estimate of the membrane capacitance and series resistance.

Solutions and drugs

The composition of the initial Krebs-Henseleit solution used for *ex vivo* experiments was (in mM): 113 NaCl, 25 $NaHCO_3$, 4.7 KCl, 1.2 $KH2PO_4$, 1.2 $MgSO_4$, 1.8 $CaCl_2$, 11 Glucose, 10 Na-Pyruvate. Isoprenaline (ISO), 3-isobutyl-1-methyl xanthine (IBMX), carbachol (CCh) were purchased from Sigma Chemical Co. (St. Louis, MO, USA). Aliquots of stock solution of ISO (1 mM) containing 1 mg ml^{-1} ascorbic acid to prevent oxidation were kept frozen. All solutions of ISO, IBMX and CCh were freshly prepared in control external solution before each experiment. To obtain the adequate concentrations in *ex vivo* experiments, the drugs were infused via a push-syringe at a 20x concentration and the infusion flow which was

adjusted to 5% of the coronary flow (estimated by continuously monitoring the volume of fluid dripping from the heart). This 5% increase in coronary flow did not modify contractility. All drugs were applied for 5 min and washed for 5 to 10 min until recovery of a new steady state.

The ionic composition of Ca^{2+}-free Tyrode's solution used for cell isolation was (in mM): NaCl 140, KCl 5.4, NaH_2PO_4 1, $MgCl_2$ 1.1, HEPES 5, Glucose 10. The pH was adjusted to 7.3 with NaOH and the solution was oxygenated. The enzymatic solution for the cardiomyocyte dissociation was composed of Ca^{2+}-free Tyrode's solution to which was added 4.05 units Collagenase D (Roche, Meylan, France), 17.8 units protease XXIV (Sigma, St Quentin Fallavier, France), 1 mg/ml BSA (ICN Pharmaceuticals, Orsay, France) and 1.4% foetal calf serum (FCS, Life Technology, Eragny/Oise, France). The 0.2-, 0.5- and 1 mM Ca^{2+}-Tyrode's solutions were composed of Ca^{2+}-free Tyrode solution to which 1.4% FCS and 0.2, 0.5 and 1 mM Ca^{2+} were respectively added. The composition of the control external solution for patch-clamp experiment was (in mM): 107.1 NaCl, 20 CsCl, 10 HEPES, 5 Glucose, 4 $NaHCO_3$, 0.8 NaH_2PO_4, 1.8 $MgCl_2$, 1.8 $CaCl_2$. The pH was adjusted to 7.4 with NaOH. Cells were exposed to different drugs with a system of capillary tubings. Patch pipettes solution contained (in mM): 119.8 CsCl, 10 HEPES, 5 EGTA, 4 $MgCl_2$, 5 Na_2CP (creatine phosphate disodium salt), 0.0062 $CaCl_2$, 3.1 Na_2ATP, 0.4 Na_2GTP. The pH was adjusted to 7.3 with CsOH.

PDE assays

Ten mice hearts were homogenized by pair (NTG) or individually (AC8TG) in 10 v/w mL buffer (20 mM Tris-HCl pH 7.5, 2.0 mM Mg acetate, 5.0 mM EGTA, 1.0 mM dithiothreitol, 10 µg/ml leupeptin, 10 µg/ml soya trypsin inhibitor, 2000 U/ml aprotinin and 0.33 mM

Pefabloc) by using an ultra-turrax (6 fold for 10 s) and a glass-glass potter homogeneizer and then stored until use in small aliquots at -80 C°.

PDE activities were measured by radioenzymatic assay as previously described (23) at a substrate concentration of 1 µM cAMP or cGMP in the presence of 15000 cpm [^{3}H]-cAMP or [^{3}H]-cGMP as a tracer, respectively. The buffer solution was of the following composition: 50 mM Tris-HCl pH 7.5, 2 mM Mg acetate, and 1 mM EGTA. Assays of total cyclic nucleotide hydrolytic activity, and isoform-specific PDE activity were run in the same batch of experiments. Tissues were diluted in order to have around 15% of hydrolysis in absence of specific inhibitors. The proportion of cAMP-hydrolyzing PDE isoforms was determined with 1 µM cAMP as substrate in the presence of 1 mM EGTA by using 10 µM rolipram for PDE4, 10 µM cilostamide for PDE3. The IBMX-sensitive cAMP-PDE activity was determined by using 100 µM IBMX. The proportion of cGMP-hydrolyzing PDE isoforms was determined with 1 µM cGMP as substrate either in basal-state (in presence of 1 mM EGTA) by using 20 µM EHNA for PDE2 or in Ca^{2+}/calmodulin-activated state (with 10 µM $CaCl_2$ and 18 nM calmodulin instead of 1 mM EGTA) by using 10 µM nimodipine for PDE1. PDE isoform-specific activities were determined as the difference between PDE activity in the absence of inhibitor and the residual hydrolytic activity observed in the presence of the selective inhibitor (5). The results were expressed as pmol.min^{-1}.mg prot^{-1}. Proteins were determined according to Lowry *et al.* (24) using bovine serum albumin as standard.

Data analysis

The results are expressed as means±SEM. Student's paired *t*-test was used to test the effect of drugs on NTG and AC8TG hearts in *ex vivo* experiments. Otherwise, Student's *t*-test for unpaired data was used to compare NTG and AC8TG mice. A value of $P<0.05$ was considered to be statistically significant.

RESULTS

β-adrenergic regulation of cardiac function

Since AC is a key enzyme mediating cardiac response to β-adrenergic stimulation, we evaluated the consequences of the cardiac expression of AC8 on the contractile response to a β-adrenergic agonist, isoprenaline (ISO). The dose-response curves to ISO were first compared in NTG and AC8TG mice under spontaneous beating condition and in 1.8 mM $[Ca^{2+}]_o$ (Fig. 1A and B). As shown earlier (1), basal LVSP and HR were much larger in AC8TG than in NTG mice (Fig. 1A and B in the absence of ISO). In NTG mice, ISO induced a classical dose-dependent stimulation of LVSP (Fig. 1A) and HR (Fig. 1B), leading to a strong increase in the cardiac work index RPP (not shown). By contrast, none of these parameters was significantly affected by β-stimulation in AC8TG mice (Fig. 1A and B).

The lack of responsiveness to ISO in AC8TG mice at 1.8 mM $[Ca^{2+}]_o$ was likely due to a saturation of the cardiac contractile machinery due to AC8 expression. Indeed, we found earlier that increasing $[Ca^{2+}]_o$ from 1.8 to 2.5 mM did not significantly change the contractility in AC8TG hearts while it strongly increased LVSP in NTG hearts (1). Therefore, we re-examined the effect of ISO at a lower $[Ca^{2+}]_o$ (1 mM), corresponding to half activation of contraction in AC8TG mice (1). These experiments were also performed under pacing conditions (at 680 bpm) to avoid any interference between HR and contractility changes. Under these new conditions, ISO (100 nM) was found to increase LVSP in both AC8TG (from 48±5 to 79±9 mmHg, n=6) and NTG mice (from 21±2 to 95±16 mmHg, n=6) (Fig. 1C). However, when expressed in relative percent variation, the ISO stimulation of LVSP was 5-fold lower in AC8TG as compared to NTG mice (64±9% vs. 340±33% increase over basal, P<0.001). As expected, ISO accelerated the onset of contraction in NTG mice and this effect

was also found in AC8TG mice, with a similar ≈15% change in +dLVSP/dt/LVSP (Fig. 1D) and t_{tp} (Fig. 1E) in both mice. ISO also exerted a net lusitropic effect in both mice (Fig. 1F and G), albeit of a larger extent in NTG (47±4% decrease of $t_{R1/2}$) than in AC8TG mice (28±4% decrease of $t_{R1/2}$, $P<0.01$, Fig. 1G). Notice that the differences in parameters observed under basal conditions between NTG and AC8TG mice were abrogated in the presence of ISO, indicating that β-adrenergic stimulation and AC8 expression affect cardiac contractility via a common pathway.

(Figure 1 near here)

Muscarinic regulation of cardiac function

We then investigated whether cardiac expression of AC8 modified the muscarinic regulation of cardiac contractility by comparing the effect of carbachol (CCh), a muscarinic receptor agonist, in NTG and AC8TG mice. As in most other mammalian species, muscarinic receptor activation had no direct negative inotropic effect in mouse ventricle as CCh (10 µM) had no effect on basal LVSP in NTG mice (-1.5±7% variation, $n=6$, Fig. 2A). However, as in other species, CCh produced a clear indirect negative inotropic effect best demonstrated after β-adrenergic receptor activation with ISO (19±5% decrease of the response to 100 nM ISO, $n=6$, $P<0.05$, Fig. 2B). This indirect effect of CCh, called 'accentuated antagonism', was also observed in AC8TG mice (Fig. 2B) with a similar amplitude (27±2% decrease of ISO response, $n=6$). However, unlike in NTG mice, CCh also produced a large and significant decrease in basal LVSP in AC8TG hearts (46±5% reduction, $n=6$). Notice that, like with ISO, CCh abrogated the difference in LVSP between NTG and AC8TG mice, indicating that muscarinic stimulation counteracts the effects of AC8 expression on cardiac contractility.

(Figure 2 near here)

Effect of PDE inhibition on cardiac function

Basal AC activity and cAMP concentration are both enhanced in the hearts of AC8TG as compared to NTG mice (21). Since cyclic nucleotide phosphodiesterases (PDE) also play a role in the control of intracellular cAMP level, we examined whether the contribution of PDE activity to the control of heart function is modified in AC8TG mice. For this, we tested the effect of IBMX, a broad-spectrum PDE inhibitor, on the contractility of paced hearts. Figure 3 shows two representative experiments performed in NTG (Fig. 3A and B) and AC8TG hearts (Fig. 3C and D) demonstrating that IBMX (10 µM) produces a positive inotropic effect in both groups of mice. On average, IBMX increased LVSP similarly by ~40% in NTG and AC8TG hearts (Fig. 3E). However, when comparing the effects of IBMX with those of ISO (Fig. 1), it appears that IBMX had a much smaller effect than a saturating concentration of ISO on contractility and kinetics in NTG mice, while IBMX and ISO produced a similar effect on all parameters in AC8TG mice (compare Fig. 3E-I to Fig. 1C-G). Thus, AC8TG mice have a higher sensitivity to PDE inhibition as compared to NTG mice which may indicate a more pronounced contribution of PDE activity to the control of heart function in this transgenic animal model.

(Figure 3 near here)

β-adrenergic regulation of basal $I_{Ca,L}$

To complement the experiments in isolated perfused heart, subsequent experiments were performed in isolated ventricular myocytes to examine how cardiac AC8 expression modifies the regulation of the L-type Ca^{2+} channel current ($I_{Ca,L}$). In our previous study (1), we found

that the basal $I_{Ca,L}$ density was similar in AC8TG and NTG mice, although the former have a several-fold increase in total AC and PKA activities (19-21). In the representative experiments shown in Fig. 4, we now find that both NTG (Fig. 4A) and AC8TG myocytes (Fig. 4B) responded to ISO (100 nM), although the effect of ISO was substantially smaller in AC8TG than in NTG mice. On average (Fig. 4C), ISO (100 nM) increased $I_{Ca,L}$ amplitude by 125±11% (n=12) in NTG and 55±8% (n=14) in AC8TG mice (P<0.05), indicating a 2-fold lower responsiveness to β-adrenergic stimulation in the transgenic mouse. This difference was not due to a reduced potency of ISO in AC8TG mice, since the 2-fold difference between the two groups remained even when ISO concentration was increased 10-fold (117.5±15.1%, n=3, in NTG vs. 46.1±9.8%, n=5, in AC8TG with 1 μM ISO). Interestingly, forskolin (10 μM), a direct activator of AC, increased $I_{Ca,L}$ amplitude by a similar amount in NTG and AC8TG mice (103±21%, n=9, and 131±21%, n=7, in NTG and AC8TG cells, respectively), comparable to the level obtained with ISO in NTG mice. This indicates that the reduced efficacy of ISO to activate $I_{Ca,L}$ in AC8TG myocytes was not due to an impairment in the PKA phosphorylation of L-type Ca^{2+} channels, but rather to a reduced coupling between β-adrenergic receptors and PKA in transgenic mice.

(Figure 4 near here)

Muscarinic regulation of $I_{Ca,L}$

In the experiments shown in Fig. 4, the 'accentuated antagonism' of CCh was examined by testing the effect of the muscarinic agonist in the presence of ISO. In both NTG (Fig. 4A) and AC8TG mice (Fig. 4B), CCh strongly antagonized the ISO response. As shown in Fig. 4D, the inhibitory effect of 1 μM CCh was similar in both groups of cells, and averaged

69.2±8.6% (*n*=5) and 77.1±9.0% (*n*=6) inhibition of the ISO (100 nM) response in NTG and AC8TG myocytes, respectively.

In addition to the 'accentuated antagonism' observed in both NTG and AC8TG mice, CCh produced a 'direct' negative inotropic effect in the isolated perfused heart of AC8TG mice only (Fig. 2). To examine whether a similar difference exists at the level of $I_{Ca,L}$, we tested the effect of CCh on basal $I_{Ca,L}$ in NTG and AC8TG mice. However, we found that CCh (1 μM) had no effect on basal $I_{Ca,L}$ in either type of mice (6±1% decrease in $I_{Ca,L}$ in NTG, *n*=4, and 4±2% in AC8TG, *n*=4).

Effect of IBMX on basal $I_{Ca,L}$

As AC8TG and NTG hearts differed in their sensitivity to PDE inhibition (Fig. 3), we examined whether isolated myocytes from NTG and AC8TG hearts also responded differently to IBMX. The rationale behind these experiments is that an increase in PDE activity might possibly explain the attenuation of $I_{Ca,L}$ response to ISO in AC8TG myocytes. As seen in the individual experiments of Fig. 5**,** a saturating concentration of IBMX (100 μM) enhanced basal $I_{Ca,L}$ in both NTG (Fig. 5A) and AC8TG (Fig. 5B) mice. However, the effect of IBMX was substantially larger in AC8TG mice. The summary data in Fig. 5C show that IBMX (100 μM) increased basal $I_{Ca,L}$ by 58±6% (*n*=15) in NTG and by 134±7% (*n*=18) in AC8TG myocytes ($P<0.05$). Thus, while ISO exerts a 2-fold lower effect in AC8TG than NTG mice, the situation is opposite with IBMX which has a 2-fold stronger effect in AC8TG than NTG mice, and forskolin acts equally well in both animals. Altogether, these results support the hypothesis that cardiac AC8 expression is counterbalanced by an increase in PDE activity, which prevents a basal activation of L-type Ca^{2+} channels and attenuates their response to β-adrenergic receptor stimulation.

(Figure 5 near here)

Measurement of PDE activity

To directly test this hypothesis, PDE activities were measured in NTG and AC8TG mice. First, the total cAMP (Table 1) and cGMP specific activities (Table 2) were determined in heart homogenates from NTG and AC8TG mice in the presence of EGTA. Basal cAMP hydrolyzing activity was increased significantly by 41% in AC8TG as compared to NTG hearts (Fig. 6A & Table 1), whereas cGMP hydrolyzing activity was decreased by 10% (Fig. 6B & Table 2), modifying markedly the ratio of cAMP- to cGMP-PDE from 1 to 1.57 (Fig. 6C).

(Figure 6 near here)

Next, we examined which PDE subtypes were involved in these alterations of cAMP and cGMP activities. To characterize the relative contribution of PDE3 and PDE4 in cAMP activity, we used cilostamide (10 µM) and rolipram (10 µM) as specific inhibitors of each subtype (5). The major cAMP hydrolytic activity was due to PDE4 which represents 58% of the total cAMP-PDE in NTG mice (Table 1). PDE4 activity increased by 28% in AC8TG hearts ($P<0.05$, Fig. 7D & Table 1). The activity of PDE3, which represents only 23% of the total cAMP hydrolytic activity in NTG hearts, was similarly increased by 27% in AC8TG heart ($P<0.05$, Fig. 7C& Table 1). Furthermore 100 µM IBMX inhibited by 77% and 80% the total cAMP hydrolytic activity in NTG and AC8TG heart homogenates, respectively, increasing by 47% ($P<0.0001$) the IBMX-sensitive cAMP-PDE activity (Table 1). The residual, IBMX-resistant hydrolytic activity, possibly due to PDE8 and PDE9 which are also

expressed in mouse heart but are resistant to inhibition by IBMX (25,26), accounted for about 20% of the total PDE activity and was not different in NTG and AC8TG hearts (Table 1).

(Table 1 near here)

Addition of 5 µM cGMP stimulated the cAMP hydrolytic activity by 81% in NTG mice but only by 27% in AC8TG mice (Table 1). Since these changes reflect a balance between cGMP-inhibition of PDE3, cGMP-activation of PDE2, and competition between cGMP and cAMP on PDE1, the difference between NTG and AC8TG mice might indicate a lower PDE2- and/or a larger PDE3+PDE1 contribution in the transgenic model. The contribution of PDE2 was evaluated with 1 µM cGMP as activator and substrate and using 20 µM EHNA as a selective inhibitor (5, 27). As shown in Table 2 and Fig. 7B, cGMP-activated PDE2 represented 79% of the total cGMP hydrolytic activity in NTG hearts but only 69% in AC8TG hearts (P<0.001).

(Figure 7 near here)

PDE1 activity is stimulated by Ca^{2+}/calmodulin (CaM), which is also an important regulator of AC8. Therefore, we determined the hydrolytic activities toward cAMP and cGMP in the presence of Ca^{2+}/CaM. Ca^{2+}/CaM-activated cAMP-PDE activity was 71% larger in AC8TG *vs.* NTG mice (P<0.0001, Table 1). The contribution of PDE1 was evaluated with 10 µM nimodipine as inhibitor (5). This increase was mainly due to a 124% increase in cAMP-PDE1 activity (P<0.0001, Table 1). In contrast, Ca^{2+}/CaM-activated cGMP-PDE activity decreased by 28% in AC8TG compared to NTG hearts (P<0.0001, Table 2), this alteration being associated with a 60% decrease in cGMP-PDE1 activity (P<0.0001, Fig. 7A and Table 2).

Table 2 also shows that other, yet unidentified, PDEs hydrolyze cGMP in mouse heart, and their contribution is substantially larger in AC8TG than NTG mice.

(Table 2 near here)

DISCUSSION

In the present report, we show that cardiac specific expression of AC8 strongly modifies the regulation of heart function by the sympathetic and parasympathetic neuromediators. Our main results can be summarized as follows: 1) the positive inotropic effect of a β-adrenergic stimulation was strongly attenuated in AC8TG mice, both at the level of the isolated heart and cardiac myocyte; 2) although CCh had no 'direct' effect on basal $I_{Ca,L}$ in either NTG or AC8TG and on contractility in NTG mice, it strongly reduced basal contractility in AC8TG hearts; 3) the 'indirect' negative inotropic effect of CCh was similar in both mice, both at the level of contractility and $I_{Ca,L}$; 4) PDE inhibition induced a more pronounced effect on contractility and $I_{Ca,L}$ in AC8TG than NTG mice; 5) this latter effect was due to an enhancement of cAMP-PDE activity in AC8TG, resulting mainly from an increase in the hydrolytic activity toward cAMP of PDE4 and PDE1 and a decrease in the hydrolytic activity toward cGMP of PDE1 and PDE2. We conclude that cardiac-expression of AC8 is accompanied by a rearrangement of PDE isoforms, leading to a strong compartmentation of the cAMP signal which shields L-type Ca^{2+} channels and protects the cardiomyocyte from deleterious Ca^{2+} overload.

Data obtained *in vivo*, after bilateral vagotomy, showed an increased basal cardiac contractility and HR in AC8TG as compared to NTG mice whereas in intact anesthetized mice, using echocardiography, HR and cardiac function were similar in both animal models (21). While the use of anesthetics may have depressed heart function alleviating the differences between the two animal models, it is also possible that an enhanced vagal tone could mask the enhanced intrinsic cardiac function in AC8TG mice. In the present study, the hearts were isolated from neural input and the circulation, allowing a more precise analysis of

the intrinsic cardiac contractile properties in response to various stimuli. Such *ex vivo* experiments unveiled a large increase in basal cardiac contractility in AC8TG as compared to NTG mice (1). Interestingly, in such conditions, CCh decreased basal cardiac contraction in AC8TG mice. This 'direct' negative inotropic effect of the muscarinic agonist, which was not observed in NTG hearts (28), reduced the contractility in AC8TG mice to the level of NTG mice, alleviating the difference in cardiac contractility between the two animal models. However, the question arises of what underlines the 'direct' negative inotropic effect of CCh in AC8TG mice? Clearly, this effect is unlikely due to a direct inhibition of AC8 by G protein α_i subunit since AC8 activity has been reported to be insensitive to G_i stimulation directly (29, 30). One possibility is that the 'direct' effect of CCh in AC8TG is due to $G\alpha_i$ inhibition of the basal activity of endogenous AC5 and/or AC6, whose contributions might be amplified by the presence of AC8. Alternatively, muscarinic regulation of basal contractility in AC8TG hearts may involve other mechanisms besides AC inhibition, such as activation of phosphatase, stimulation of cGMP-stimulated PDE2 or phosphorylation via cGMP-dependent protein kinase (see ref. 31 for a review). In particular, the two latter processes may be amplified in AC8TG hearts due to the reduced cGMP hydrolytic activity observed in this study.

Our previous *in vivo* study showed that cardiac function was not affected by β-adrenergic stimulation in AC8TG hearts (21). Similarly, we found in this *ex vivo* study that AC8TG hearts did not respond to ISO when tested at near physiological (1.8 mM) Ca^{2+} concentration. However, ISO produced a clear positive inotropic effect in AC8TG mice when the external Ca^{2+} concentration was reduced to 1 mM, i.e. a concentration at which cardiac contraction is half maximal (1). This indicates that the β-adrenergic signaling pathway was still functional in AC8TG mice but that the lack of ISO effect at higher Ca^{2+} concentrations was due to a saturation of the contractile machinery. Consistent with this hypothesis, we found earlier that increasing $[Ca^{2+}]_o$ from 1.8 to 2.5 mM did not significantly change the contractility in AC8TG

hearts while it strongly increased LVSP in NTG hearts (1). Interestingly, cardiac function was no longer different in NTG and AC8TG hearts upon a maximal β-adrenergic stimulation with ISO. This confirms our hypothesis that AC8 expression and β-adrenergic stimulation share a common pathway to produce a positive inotropic effect. It should be noted that the positive inotropic effect of ISO in AC8TG hearts is unlikely to result from a stimulation of AC8 by G protein α_s subunits since AC8 activity has been reported to be insensitive to G_s stimulation (30). More likely, the positive inotropic effect of ISO in AC8TG mice observed in *ex vivo* experiments reflects the stimulation of endogenous cardiac AC5 and/or AC6 cyclase activity.

Since the quantity of AC5 and AC6 proteins and β-adrenergic receptors was not altered in AC8TG (21), one might expect, at first approximation, that $G\alpha_s$ stimulation of these endogenous adenylyl cyclases would generate similar responses in AC8TG and NTG mice. Our electrophysiological experiments in isolated myocytes clearly showed that this was not the case. Indeed, the response of $I_{Ca,L}$ to ISO was 2-fold lower in AC8TG vs. NTG mice, although the response to forskolin was identical demonstrating a comparable sensitivity to PKA phosphorylation of L-type Ca^{2+} channels in the two type of mice. This suggests that a mechanism prevents Ca^{2+} channels in AC8TG mouse from an excessive stimulation by cAMP. Hyperactivation of G_i protein pathways was unlikely to account for such mechanism, as the muscarinic regulation of $I_{Ca,L}$, both at basal and ISO-stimulated level, was similar in AC8TG and NTG mice. A possible mechanism could be an inhibition of endogenous AC activity in AC8TG mice as a result of the increase in PKA activity. Indeed, both AC5 and AC6 are directly phosphorylated and inhibited by PKA (5, 6, 29, 32, 33). Phosphorylation by PKA inhibits AC5 activity by decreasing the maximal velocity of the enzyme (33). More interestingly, phosphorylation of AC6 would disrupt the functional $G\alpha_s$ binding site, leading to an attenuation of its stimulation by $G\alpha_s$ coupled receptor (32). Although attractive, such a PKA-mediated AC inhibition might not easily explain our data. Indeed, if one assumes that in

AC8TG mice the ISO effect on $I_{Ca,L}$ is reduced due to a PKA inhibition of AC5/AC6 activity, then one would expect the same pool of PKA to phosphorylate Ca^{2+} channels and activate basal $I_{Ca,L}$. However, as shown in our previous study, basal $I_{Ca,L}$ is not increased in AC8TG mice (1) indicating that L-type Ca^{2+} channels are not in contact with the cAMP/PKA pathway initiated at AC8.

Since cAMP level is not only controlled by its production but also by its degradation (5-7, 29), we examined the possibility that the contribution of PDE activity might be modified in AC8TG mice. Several observations led us to conclude that PDE activity is up-regulated in transgenic mice. First, application of IBMX, a broad-spectrum PDE inhibitor, increased cardiac function in AC8TG as well as in NTG mice, but the kinetic parameters were modified in AC8TG hearts only. Moreover, the same concentration of IBMX increased LVSP maximally in AC8TG hearts, to the level reached by a maximal concentration of ISO, but not in NTG hearts. Thus, AC8TG mice appeared more sensitive to PDE inhibition than NTG mice. Second, at the cellular level, application of IBMX induced a 2-fold larger stimulation of $I_{Ca,L}$ in AC8TG than NTG myocytes. This was as if PDE inhibition "revealed" the presence of AC8 to L-type Ca^{2+} channels. Finally, PDE assay confirmed the enhancement of cAMP hydrolytic activity of these enzymes in AC8TG and their increased sensitivity to IBMX. This increase in PDE activity was essentially due to an increase in PDE4 and Ca^{2+}/CaM-activated PDE1 hydrolytic activity toward cAMP. As shown earlier (34), the expression of PDE isoforms might be directly controlled by the level of cAMP. Surprisingly, while we found an increase in Ca^{2+}/CaM-activated PDE1 hydrolytic activity toward cGMP, we found at the same time a decrease in Ca^{2+}/CaM-activated PDE1 hydrolytic activity toward cGMP in AC8TG hearts. One possible explanation for this apparent discrepancy is that the overall PDE1 activity corresponds to the activity of different PDE1 isoforms, such as PDE1A and PDE1C which differ in their kinetic constants as previously characterized in rat heart (35). The

expression of PDE splice variants might also differ between NTG and AC8TG mice and this may contribute to the overall increase in cAMP-PDE activity. We believe that this up-regulation of cAMP-PDE activity is a compensatory mechanism to AC8 expression, which serves a protective role by shielding L-type Ca^{2+} channels, hence preventing an excessive and deleterious entry of Ca^{2+} into the cell.

Such a contribution of PDE to the compartmentation of cAMP signaling pathway has already been reported. In frog myocyte, during ISO-stimulation of $I_{Ca,L}$, PDE activity was shown to limit the cAMP broadcast throughout the cell, hence resulting in a local β-adrenergic regulation of this current (18, 36, 37) . It has been shown that PDE3 and PDE4 are differently associated to subcellular structures in cardiac tissues: PDE4 is associated to sarcolemma (38), and nuclear envelope (40) whereas PDE3 is mainly associated to sarcoplasmic reticulum (41). Thus, PDE3 and PDE4 might locally regulate cAMP level in the vicinity of functional proteins regulated by cAMP-dependent protein kinase (42). In AC8TG ventricular myocytes, an increase in PDE activity and particularly in PDE4 may play a role in limiting the spatial spread of cAMP which dissociates $I_{Ca,L}$ from AC8 protein and also reduces β-adrenergic stimulation of this current. Moreover, it was shown in cardiac ventricle that rolipram, a selective PDE4 inhibitor, although increasing cAMP level, was unable to affect the phosphorylation state of phospholamban and the inhibitory subunit of troponin, supporting the role of PDE4 in cAMP compartmentation (43). Many proteins may be involved in this spatial cAMP signal localization. A-kinase anchoring proteins (AKAP) have been shown to localize PKA near its target proteins during ß-adrenergic regulation of cardiac contractility (44). Similar proteins were also shown to anchor PDE4 isoforms at specific organelles (45, 46). Finally, recent studies have emphasized the role of caveolae in the spatial organization of various signaling complexes, which might facilitate the interaction between molecules and contribute to the localization of the cAMP signal in a restrictive place (14, 47, 48).

In conclusion, our study demonstrates that PDEs play a dynamic role in shaping the spatial profile of intracellular cAMP concentration in cardiac myocytes. Although cAMP is a relatively small molecule which should readily diffuse throughout the cell, we propose that its concentration is different in different cellular compartments (36). In the unique model of the AC8TG mouse, the overall intracellular cAMP concentration is much increased (21), but not necessarily in all compartments. For instance, the degree of cAMP-dependent phosphorylation may be increased for proteins located at the sarcoplasmic reticulum membrane (e.g. phospholamban, ryanodine receptor) and/or in the contractile machinery (e.g. troponin I), accounting for the strong positive inotropic and lusitropic effect seen in AC8TG mice, both at the level of the whole heart and single myocyte (1). However, the degree of cAMP-dependent phosphorylation may remain normal, or even become lower during β-adrenergic stimulation, for sarcolemmal L-type Ca^{2+} channels, which might explain why the AC8TG mice survive and show no phenotypic alteration or any sign of hypertrophy or cardiomyopathy (1, 21). Thus, activation of cAMP-PDE may serve a protective role during a long-term activation of the cAMP cascade.

Acknowledgements

We thank Patrick Lechêne for skilful programming of the automated data analysis, Florence Lefebvre and Hélène Basaran for excellent technical help.

Table 1: cAMP-PDE activity

	NTG	% total	AC8TG	% total	AC8TG *vs.* NTG
Basal	91±3	100	128±7	100	↑+41%
PDE3 (cilostamide)	21±2	23	27±1	21	↑+27%
PDE4 (rolipram)	52±1	58	67±1	52	↑+28%
other PDEs[1]	18±2	19	34±3	27	↑+101%
IBMX-sensitive	70±3	77	103±5	80	↑+47%
IBMX-resistant[2]	21±2	23	25±2	20	n.s.
cGMP-activated	164±4	181	163±4	127	n.s.
Ca^{2+}/CaM-activated	108±3	100	185±8	100	↑+71%
PDE1 (nimodipine)	41±2	38	92±5	50	↑+124%

Basal cAMP-PDE activity was determined with 1 µM cAMP as substrate in the presence of 1 mM EGTA. PDE3 activity was obtained using 10 µM cilostamide. PDE4 activity was obtained using 10 µM rolipram. The IBMX-sensitive PDE activity was determined using 100 µM IBMX. Cyclic GMP activated state was obtained by adding 5 µM cGMP. Ca^{2+}/CaM-activated state was obtained with 10 µM $CaCl_2$ and 18 nM calmodulin (CaM) instead of 1 mM EGTA. PDE1 activity was obtained using 10 µM nimodipine. PDE1, PDE3, PDE4 and IBMX-sensitive activities were determined as the difference between PDE activity in the absence of inhibitor and the residual hydrolytic activity observed in the presence of the inhibitor. The results are expressed in $pmol.min^{-1}.mg\ prot^{-1}$ as mean values ± SEM of 10 hearts homogenized by pair (NTG) or individually (AC8TG). All differences between AC8TG and NTG hearts are statistically significant at least at $P<0.05$ unless specified. n.s., non significant. [1]Calculated value obtained as: basal PDE-(PDE3+PDE4). [2]Calculated value obtained as: basal PDE-(IBMX-sensitive).

Table 2: cGMP-PDE activity

	NTG	% total	AC8TG	% total	AC8TG *vs.* NTG
Basal	91±3	100	82±2	100	↓-10%
PDE2 (EHNA)	73±2	79	57±2	69	↓-21%
other PDEs[1]	18±0	20	25±1	31	↑+37%
Ca^{2+}/CaM-activated	228±9	100	164±1	100	↓-28%
PDE1 (nimodipine)	103±5	45	41±7	25	↓-60%
other PDEs[2]	52±3	23	66±3	40	↑+26%

Basal cGMP-PDE activity was determined with 1 µM cGMP as substrate in the presence of 1 mM EGTA. PDE2 activity was obtained using 20 µM EHNA. Ca^{2+}/CaM-activated state was obtained with 10 µM $CaCl_2$ and 18 nM calmodulin (CaM) instead of 1 mM EGTA. PDE1 activity was obtained using 10 µM nimodipine. PDE1 and PDE2 activities were determined as the difference between PDE activity in the absence of inhibitor and the residual hydrolytic activity observed in the presence of the inhibitor. The results are expressed in $pmol.min^{-1}.mg\ prot^{-1}$ as mean values ± SEM of 10 hearts homogenized by pair (NTG) or individually (AC8TG). All differences between AC8TG and NTG hearts summarized on the last column are statistically significant at least at $P<0.05$ unless specified. n.s., non significant. [1]Calculated value obtained as: basal PDE-(PDE2). [2]Calculated value obtained as: Ca^{2+}/CaM-activated PDE-(PDE2+PDE1).

REFERENCES

1. Georget, M., Mateo, P., Vandecasteele, G., Jurevicius, J., Lipskaia, L., Defer, N., Hanoune, J., Hoerter, J., and Fischmeister, R. Augmentation of cardiac contractility with no change in L-type Ca^{2+} current in transgenic mice with a cardiac-directed expression of the human adenylyl cyclase type 8 (AC8). *FASEB Journal* express article 10.1096/fj.02-0292fje. Published online August 21, 2002

2. Rapundalo, S. T. (1998) Cardiac protein phosphorylation: functional and pathophysiological correlates. *Cardiovasc. Res.* **38,** 559-588

3. Méry, P. F., Abi-Gerges, N., Vandecasteele, G., Jurevicius, J., Eschenhagen, T., and Fischmeister, R. (1997) Muscarinic regulation of the L-type calcium current in isolated cardiac myocytes. *Life Sciences* **60,** 1113-1120

4. Brodde, O. E. and Michel, M. C. (1999) Adrenergic and muscarinic receptors in the human heart. *Pharmacol. Rev.* **51,** 651-689

5. Stoclet, J.-C., Keravis, T., Komas, N., and Lugnier, C. (1995) Cyclic nucleotide phosphodiesterases as therapeutic targets in cardiovascular diseases. *Exp. Opin. Invest. Drugs* **4,** 1081-1100

6. Conti, M. and Jin, S.L.C. (2000) The molecular biology of cyclic nucleotide phosphodiesterases. *Progress in Nucleic Acid Research and Molecular Biology* **63,** 2-33

7. Beavo, J. A. (1995) Cyclic nucleotide phosphodiesterases: Functional implications of multiple isoforms. *Physiol. Rev.* **75,** 725-748

8. Verde, I., Vandecasteele, G., Lezoualc'h, F., and Fischmeister, R. (1999) Characterization of the cyclic nucleotide phosphodiesterase subtypes involved in the regulation of the L-type Ca^{2+} current in rat ventricular myocytes. *Br. J. Pharmacol.* **126,**

9. Brunton, L. L., Hayes, J. S., and Mayer, S. E. (1979) Hormonally specific phosphorylation of cardiac troponin I and activation of glycogen phosphorylase. *Nature* **280,** 78-80

10. Buxton, I. L. O. and Brunton, L. L. (1983) Compartments of cyclic AMP and protein kinase in mammalian cardiomyocytes. *J. Biol. Chem.* **258,** 10233-10239

11. Hayes, J. S., Brunton, L. L., Brown, J. H., Reese, J. B., and Mayer, S. E. (1979) Hormonally specific expression of cardiac protein kinase activity. *Proc. Natl. Acad. Sci. USA* **76,** 1570-1574

12. Vila Petroff, M. G., Egan, J. M., Wang, X., and Sollott, S. J. (2001) Glucagon-like peptide-1 increases cAMP but fails to augment contraction in adult rat cardiac myocytes. *Circ. Res.* **89,** 445-452

13. Bers, D. M. and Ziolo, M. T. (2001) When Is cAMP Not cAMP? Effects of Compartmentalization. *Circ. Res.* **89,** 373-375

14. Steinberg, S. F. and Brunton, L. L. (2001) Compartmentation of G protein-coupled signaling pathways in cardiac myocytes. *Annu. Rev. Pharmacol. Toxicol.* **41,** 751-773

15. Xiao, R. P., Cheng, H. P., Zhou, Y. Y., Kuschel, M., and Lakatta, E. G. (1999) Recent advances in cardiac β_2-adrenergic signal transduction. *Circ. Res.* **85,** 1092-1100

16. Steinberg, S. F. (1999) The molecular basis for distinct β-adrenergic receptor subtype actions in cardiomyocytes. *Circ. Res.* **85,** 1101-1111

17. Xiao, R. P., Hohl, C., Altschuld, R., Jones, L., Livingston, B., Ziman, B., Tantini, B., and Lakatta, E. G. (1994) β_2-adrenergic receptor-stimulated increase in cAMP in rat heart cells is not coupled to changes in Ca^{2+} dynamics, contractility, or phospholamban phosphorylation. *J. Biol. Chem.* **269,** 19151-19156

18. Kueschel, M., Zhou, Y.Y., Cheng, H., Zhang, S.J., Chen, Y., Lakatta, E.G., and Xiao, R.P. (1999) Gi protein-mediated functional compartmentalization of cardiac β_2-adrenergic signaling. *J. Biol. Chem.* **274,** 22048-22052

19. Cali, J. J., Zwaagstra, J. C., Mons, N., Cooper, D. M., and Krupinski, J. (1994) Type VIII adenylyl cyclase. A Ca^{2+}/calmodulin-stimulated enzyme expressed in discrete regions of rat brain. *J. Biol. Chem.* **269,** 12190-12195

20. Defer, N., Marinx, O., Stengel, D., Danisova, A., Iourgenko, V., Matsuoka, I., Caput, D., and Hanoune, J. (1994) Molecular cloning of the human type VIII adenylyl cyclase. *FEBS Lett.* **351,** 109-113

21. Lipskaia, L., Defer, N., Esposito, G., Hajar, I., Garel, M. C., Rockman, H. A., and Hanoune, J. (2000) Enhanced cardiac function in transgenic mice expressing a Ca^{2+}-stimulated adenyl cyclase. *Circ. Res.* **86,** 795-801

22. Wolska, B. M. and Solaro, R. J. (1996) Method for isolation of adult mouse cardiac myocytes for studies of contraction and microfluorimetry. *Am. J. Physiol. Heart & Circulatory Physiol.* **40,** H1250-H1255

23. Keravis, T. M., Wells, J. N., and Hardman, J. G. (1980) Cyclic nucleotide phosphodiesterase activities from pig coronary arteries: lack of interconvertibility of majors forms. *Biochim. Biophys. Acta* **613,** 116-129

24. Lowry, O. H., Rosebrough, N. J., Farr, A. L., and Randall, R. J. (1951) Protein measurement with the folin phenol reagent. *J. Biol. Chem.* **193,** 265-275

25. Fisher, D. A., Smith, J. F., Pillar, J. S., St Denis, S. H., and Cheng, J. B. (1998). Isolation and characterization of PDE9A, a novel human cGMP-specific phosphodiesterase. *J. Biol. Chem.* **273**, 15559-15564

26. Soderling, S. H., Bayuga, S. J., and Beavo, J. A. (1998). Cloning and characterization of a cAMP-specific cyclic nucleotide phosphodiesterase. *Proc Natl Acad Sci USA* **95**, 8991-8996

27. Méry, P. F., Pavoine, C., Pecker, F., and Fischmeister, R. (1995). Erythro-9-(2-hydroxy-3-nonyl)adenine inhibits cyclic GMP-stimulated phosphodiesterase in isolated cardiac myocytes. *Mol. Pharmacol.* **48**, 121-130.

28. Vandecasteele, G., Eschenhagen, T., Scholz, H., Stein, B., Verde, I., and Fischmeister, R. (1999) Muscarinic and β-adrenergic regulation of heart rate, force of contraction and calcium current is preserved in mice lacking endothelial nitric oxide synthase. *Nature Medicine* **5,** 331-334

29. Defer, N., Best-Belpomme, M., and Hanoune, J. (2000) Tissue specificity and physiological relevance of various isoforme of adenylyl cyclase. *Am. J. Physiol. Renal Physiol.* **279,** F400-F416

30. Nielsen, M. D., Chan, G. C. K., Poser, S. W., and Storm, D. R. (1996) Differential regulation of type I and type VIII Ca^{2+}-stimulated adenylyl cyclase by Gi-coupled receptors *in vivo*. *J. Biol. Chem.* **271,** 33308-33316

31. Dhein, S., Van Koppen, C. J., and Brodde, O. E. (2001). Muscarinic receptors in the mammalian heart. *Pharmacol. Res.* **44**, 161-182

32. Chen, Y., Harry, A., Li, J., Smit, M. J., Bai, X., Magnusson, R., Pieroni, J. P., Weng, G., and Iyengar, R. (1997) Adenylyl cyclase 6 is selectively regulated by protein kinase a phosphorylation in a region involved in G_α stimulation. *Proc. Natl. Acad. Sci. USA* **94,** 14100-14104

33. Iwami, G., Kawabe, J. I., Ebina, T., Cannon, P. J., Homcy, C. J., and Ischikawa, Y. (1995) Regulation of Adenylyl Cyclase by Protein Kinase A. *J. Biol. Chem.* **270,** 12481-12484

34. Jiang, X., Paskind, M., Weltzien, R., and Epstein, P. M. (1998). Expression and regulation of mRNA for distinct isoforms of cAMP-specific PDE-4 in mitogen-stimulated and leukemic human lymphocytes. *Cell. Biochem. Biophys.* **28**, 135-160

35. Sonnenburg W. K., Rybalkin S. D., Bornfeldt K. E., Kwak K. S., Rybalkina I. G., and Beavo J. A. (1998) Identification, quantification, and cellular localization of PDE1 calmodulin-stimulated cyclic nucleotide phosphodiesterases. *Methods* **14**, 3-19.

36. Jurevicius, J. and Fischmeister, R. (1996) cAMP compartmentation is responsible for a local activation of cardiac Ca^{2+} channels by β-adrenergic agonists. *Proc. Natl. Acad. Sci. USA* **93,** 295-299

37. Hohl, C. M. and Li, Q. (1991) Compartmentation of cAMP in Adult Canine Ventricular Myocytes - Relation to Single-Cell Free Ca^{2+} Transients. *Circ. Res*. **69,** 1369-1379

38. Okruhlicova, L., Tribulova, N., Eckly, A., and Lugnier, C. (1996) Cytochemical distribution of cyclic AMP-dependent 3', 5'-nucleotide phosphodiesterase in the rat myocardium. *Histochemistry Journal* **28,** 165-172

39. Okruhlicova, L., Vrbjar, N., and Lugnier, C. (1998) Charactrization of type 4 cyclic nucleotide phosphodiesterase (PDE4) in cardiac sarcolemma. *Exp. Clin. Cardiol.* **3,** 188-192

40. Lugnier, C., Keravis, T., Le Bec, A., Pauvert, O., Proteau, S., and Rousseau, E. (1999) Characterization of cyclic nucleotide phosphodiesterase isoforms associated to isolated cardiac nuclei. *Biochim. Biophys. Acta* **1472,** 431-446

41. Lugnier, C., Muller, B., Le Bec, A., Beaudry, C., and Rousseau, E. (1993) Characterization of indolidan-sensitive and rolipram-sensitive cyclic nucleotide phosphodiesterases in canine and human cardiac microsomal fractions. *J. Pharm. Exp. Ther*. **265,** 1142-1151

42. Eckly-Michel, A., Martin, V., and Lugnier, C. (1997) Involvement of cyclic nucleotide-dependent protein kinases in cyclic AMP-mediated vasorelaxation. *Br. J. Pharmacol.* **122,** 158-164

43. Boknik, P., Neumann, J., Schmitz, W., Scholz, H., and Wenzlaff, H. (1997) Characterization of biochemical effects of CGS 21680C, an A2-adenosine receptor agonist, in the mammalian ventricle. *J. Cardiovasc. Pharmacol.* **30,** 750-758

44. Fink, M. A., Zakhary, D. R., Mackey, J. A., Desnoyer, R. W., AppersonHansen, C., Damron, D. S., and Bond, M. (2001) AKAP-mediated targeting of protein kinase A regulates contractility in cardiac myocytes. *Circ. Res.* **88,** 291-297

45. Dodge, K. L., Khouangsathiene, S., Kapiloff, M. S., Mouton, R., Hill, E. V., Houslay, M. D., Langeberg, L. K., and Scott, J. D. (2001) mAKAP assembles a protein kinase A/PDE4 phosphodiesterase cAMP signaling module. *EMBO J.* **20,** 1921-1930

46. Verde, I., Pahlke, G., Salanova, M., Zhang, G., Wang, S., Coletti, D., Onuffer, J., Jin, S. L. C., and Conti, M. (2001) Myomegalin is a novel protein of the Golgi/centrosome that interacts with a cyclic nucleotide phosphodiesterase. *J. Biol. Chem.* **276,** 11189-11198

47. Rybin, V. O., Xu, X., Lisanti, M. P., and Steinberg, S. F. (2000) Differential targeting of ß-adrenergic receptor subtypes and adenylyl cyclase to cardiomyocyte caveolae: a mechanism to functionally regulate the cAMP signaling pathway. *J. Biol. Chem.* **275,** 41447-41457

48. Shaul, P. W., and Anderson, R. G. W. (1998) Role of plasmalemmal caveolae in signal transduction. *Am. J. Physiol. Lung Cell. Mol. Physiol.* **19,** L843-L851

FIGURE LEGENDS

Figure 1. β-adrenergic regulation of cardiac function *in* NTG and AC8TG mice. In *A* and *B*, the hearts were spontaneously beating and perfused with 1.8 mM $[Ca^{2+}]_o$. Increasing concentrations of isoprenaline (ISO) were added to the perfusate while continuously measuring left ventricular systolic pressure (LVSP, *A*) and heart rate (HR, *B*) in NTG (○) and AC8TG mice (▲). The points are means±SEM. NTG, *n*=6; AC8TG, *n*=5. * *P*<0.05 and ** *P*<0.01 versus NTG. Next (*C* to *G*), the hearts were stimulated at 680 bpm and perfused with 1 mM $[Ca^{2+}]_o$ in the absence (*empty bars*) or presence (*filled bars*) of 100 nM isoprenaline (ISO). LVSP (*C*), the maximal rate of contraction (+dLVSP/dt/LVSP, *D*), the time to peak of contraction (t_{tp}, *E*), the maximal rate of relaxation (-dLVSP/dt/LVSP, *F*) and the time for half relaxation ($t_{R1/2}$, *G*) were measured in each condition in NTG and AC8TG mice, as indicated. The bars are means±SEM. NTG, *n*=6; AC8TG, *n*=6. * *P*0.05, ** *P*<0.01 and *** *P*<0.001 ISO versus control.

Figure 2. Muscarinic regulation of cardiac contraction in NTG and AC8TG mice. The hearts were stimulated at 680 bpm and perfused with 1 mM $[Ca^{2+}]_o$. (*A*) Mean of 6 NTG and 6 AC8TG hearts are represented in the absence (*empty bars*) or presence (*filled bars*) of 10 µM carbachol (CCh). (*B*) Mean of 6 NTG and 6 AC8TG ISO-stimulated hearts are represented in the absence (*empty bars*) or presence (*filled bars*) of 10 µM CCh. The bars are means±SEM. * *P*<0.05 and ** *P*<0.01 AC8TG versus NTG (paired *t*-test).

Figure 3. Cardiac response to IBMX in NTG and AC8TG mice. On the top, original recordings of left ventricular contraction of NTG (*A, B*) and AC8TG (*C, D*) hearts under basal conditions (*A, C*) and after application of 10 µM IBMX (*B, D*). The hearts were stimulated at 680 bpm and perfused at 1 mM $[Ca^{2+}]_o$. (*E* to *I*) Mean results of 6 NTG and 6 AC8TG hearts are compared in the absence (*empty bars*) or presence (*filled bars*) of 10 µM IBMX. LVSP (*E*), the maximal rate of contraction (+dLVSP/dt/LVSP, *F*), the time to peak of contraction (t_{tp}, *G*) , the maximal rate of relaxation (-dLVSP/dt/LVSP, *H*) and the time for half relaxation ($t_{R1/2}$, *I*) were measured in each condition in NTG and AC8TG mice. The bars are means±SEM. * *P*<0.05 and ** *P*<0.01 IBMX versus control.

Figure 4. **β-adrenergic and muscarinic regulation of $I_{Ca,L}$ in NTG and AC8TG ventricular myocytes.** The ventricular myocytes from NTG (*A*) and AC8TG mice (*B*) were first exposed to the control external solution and the solid lines indicate the period of drug perfusion. Each symbol corresponds to a measure of $I_{Ca,L}$ at 0 mV obtained every 8 s (holding potential of -50 mV). The individual current traces shown on top of the graphs were recorded at the times indicated by the corresponding letters in the bottom graphs. The mean effects of ISO or forskolin (10 µM) on $I_{Ca,L}$ and of CCh on ISO-stimulated $I_{Ca,L}$ in NTG (*empty bars*) and AC8TG mice (*filled bars*) are shown in *C* and *D*, respectively. The bars indicate the means and the lines the SEM of the number of cells given. * *P*< 0.001 *vs.* NTG.

Figure 5. Effect of IBMX on $I_{Ca,L}$ in NTG and AC8TG ventricular myocytes. The ventricular myocytes from NTG (*A*) and AC8TG mice (*B*) were first exposed to the control external solution. During the periods indicated by the solid lines, the cells were superfused by 100 µM of IBMX. Each symbol corresponds to a measure of $I_{Ca,L}$ at 0 mV obtained every 8 s (holding potential of -50 mV). The individual current traces shown on top of the graphs were

recorded at the times indicated by the corresponding letters in the bottom graphs. (*C*) Mean effects of IBMX on $I_{Ca,L}$ in NTG (*empty bar*) and AC8TG mice (*filled bar*). The bars indicate the means and the lines the SEM of the number of cells given. * $P< 0.001$ *vs.* NTG.

Figure 6. Cardiac phosphodiesterase activity in NTG and AC8TG mice. The results are expressed as $pmol.min^{-1}.mg\ prot^{-1}$ and represent the mean results from 10 hearts homogenized by pair (NTG, *empty bars*) or individually (AC8TG, *filled bars*). The bars indicate the means and the lines the SEM. * $P<0.05$, ** $P<0.01$ and *** $P<0.001$ *vs.* NTG.

Figure 7. Cardiac PDE specific isoform activities in NTG and AC8TG mice. The results are expressed as $pmol.min^{-1}.mg\ prot^{-1}$ and represent the mean results from 10 hearts homogenized by pair (NTG, *empty bars*) or individually (AC8TG, *filled bars*). To identify the specific PDE isoform activities, selective PDE inhibitors were added: 10 µM nimodipine for PDE1 (*A*), 20 µM EHNA for PDE2 (*B*), 10 µM cilostamide for PDE3 (*C*) and 10 µM rolipram for PDE4 (*D*). The bars indicate the means and the lines the SEM. * $P<0.05$ and *** $P<0.001$ *vs.* NTG.

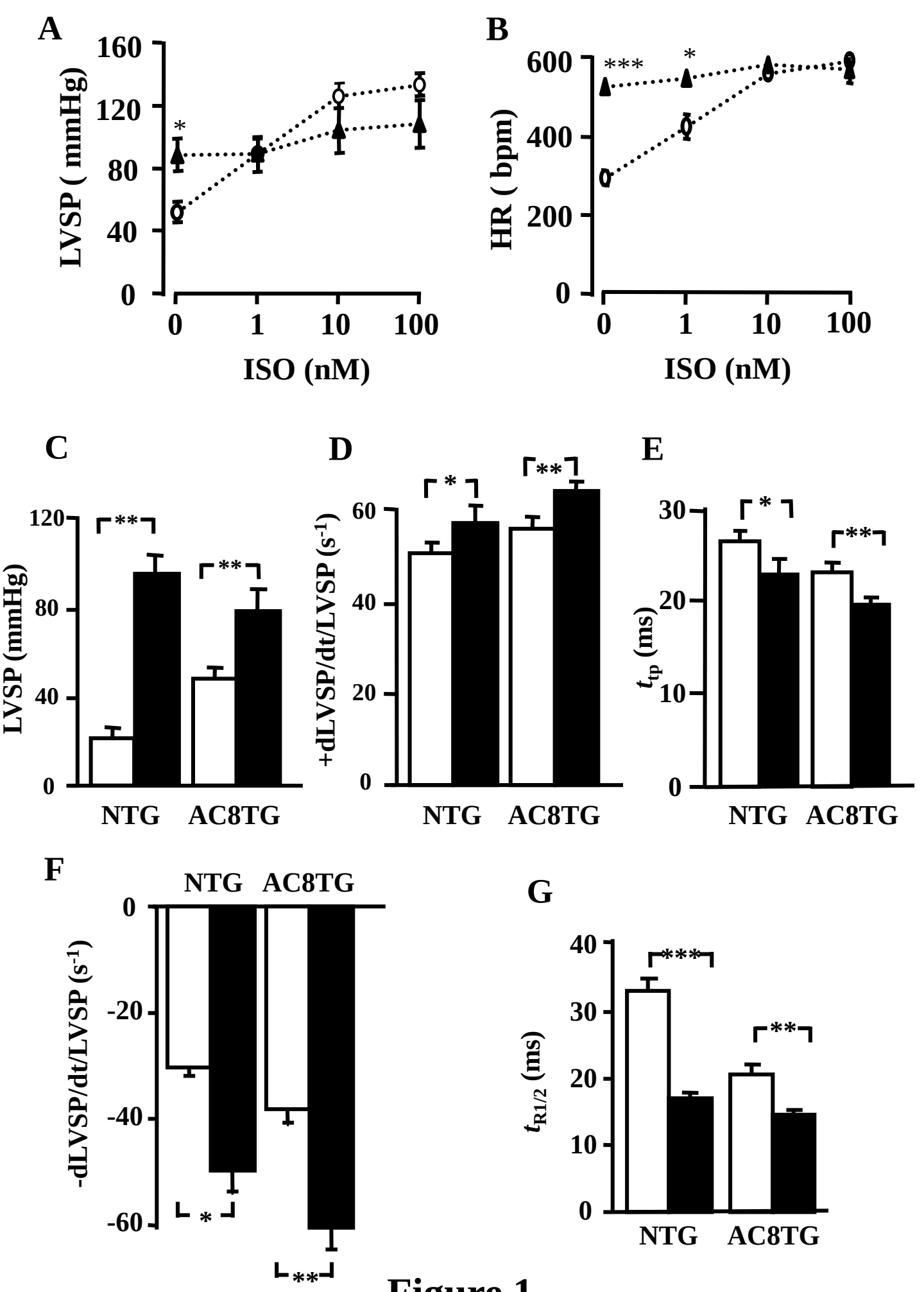
A
LVSP (mmHg)
160
120
80
40
0
*
0
1
10
100
ISO (nM)
B
HR (bpm)
600
400
200
0
***
*
0
1
10
100
ISO (nM)
C
LVSP (mmHg)
120
80
40
0
**
**
NTG
AC8TG
D
+dLVSP/dt/LVSP (s-1)
60
40
20
0
*
**
NTG
AC8TG
E
ttp (ms)
30
20
10
0
*
**
NTG
AC8TG
F
NTG
AC8TG
-dLVSP/dt/LVSP (s-1)
0
-20
-40
-60
*
**
G
tR1/2 (ms)
40
30
20
10
0
***
**
NTG
AC8TG

Figure 1

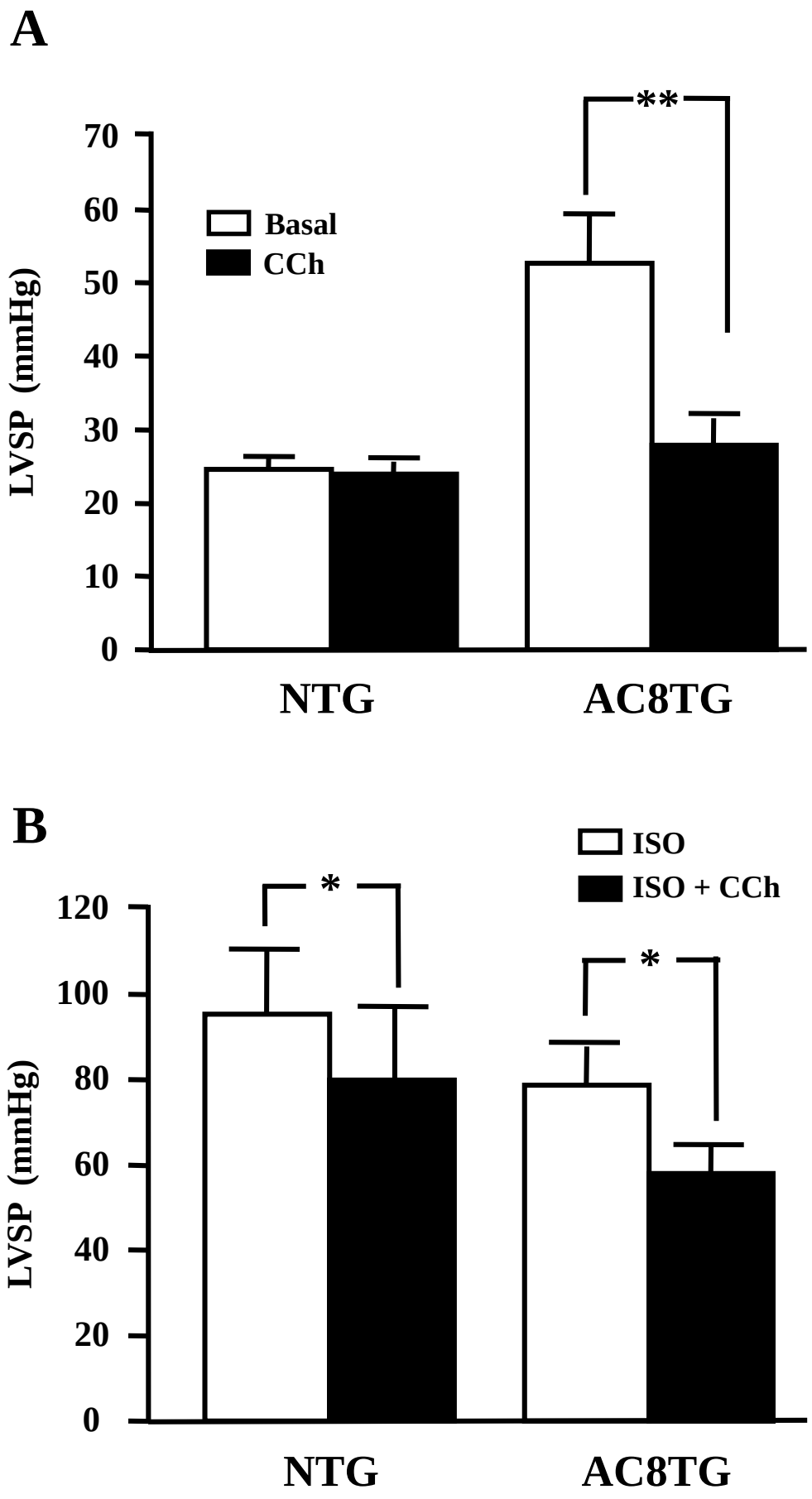
A
LVSP (mmHg)
70
60
50
40
30
20
10
0
Basal
CCh
**
NTG
AC8TG
B
LVSP (mmHg)
120
100
80
60
40
20
0
ISO
ISO + CCh
*
*
NTG
AC8TG

Figure 2

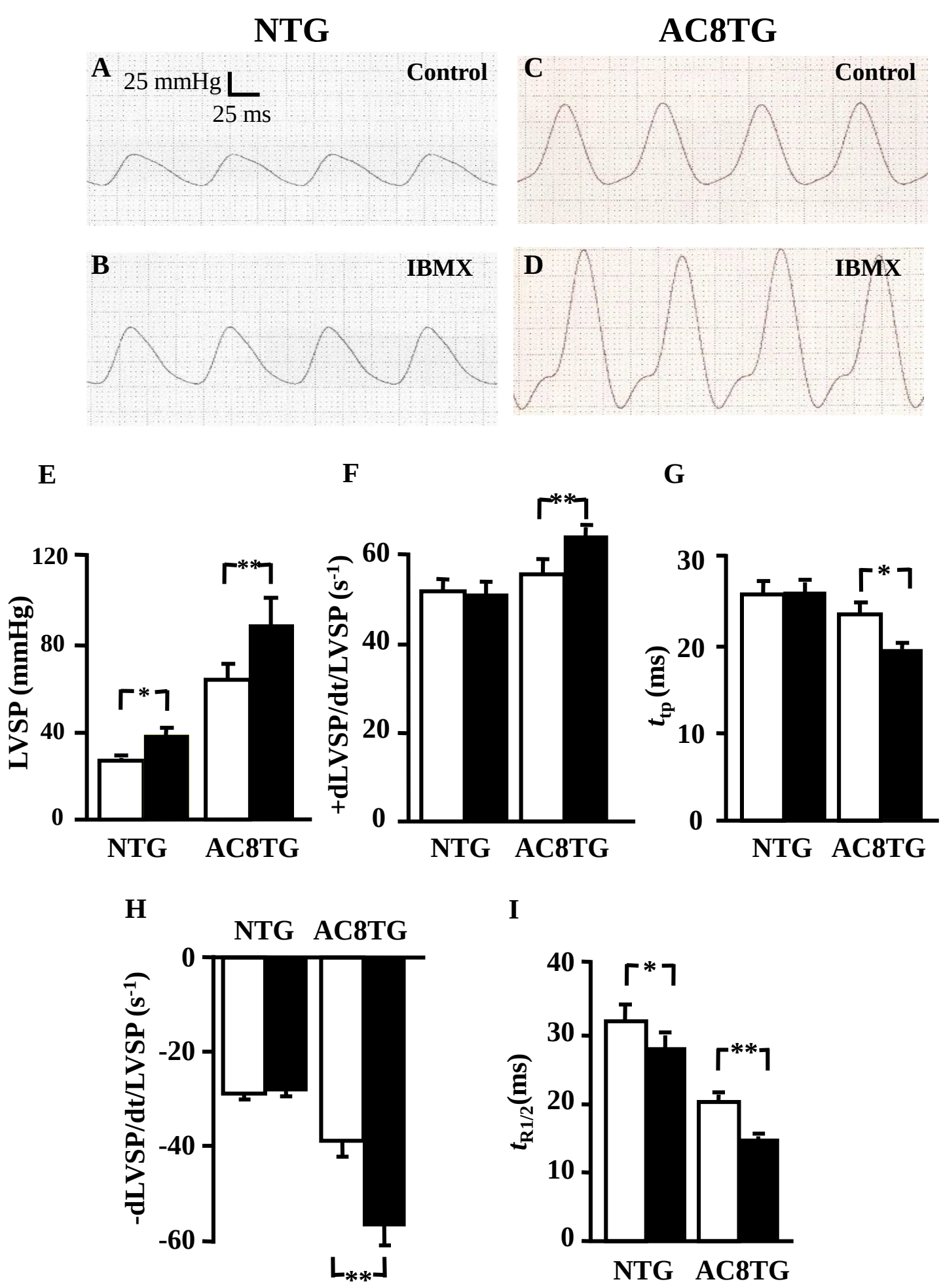
NTG
AC8TG
A
25 mmHg
25 ms
Control
C
Control
B
IBMX
D
IBMX
E
LVSP (mmHg)
120
80
40
0
*
**
NTG
AC8TG
F
+dLVSP/dt/LVSP (s-1)
60
40
20
0
**
NTG
AC8TG
G
tp (ms)
30
20
10
0
*
NTG
AC8TG
H
NTG
AC8TG
-dLVSP/dt/LVSP (s-1)
0
-20
-40
-60
**
I
tR1/2(ms)
40
30
20
10
0
*
**
NTG
AC8TG

Figure 3

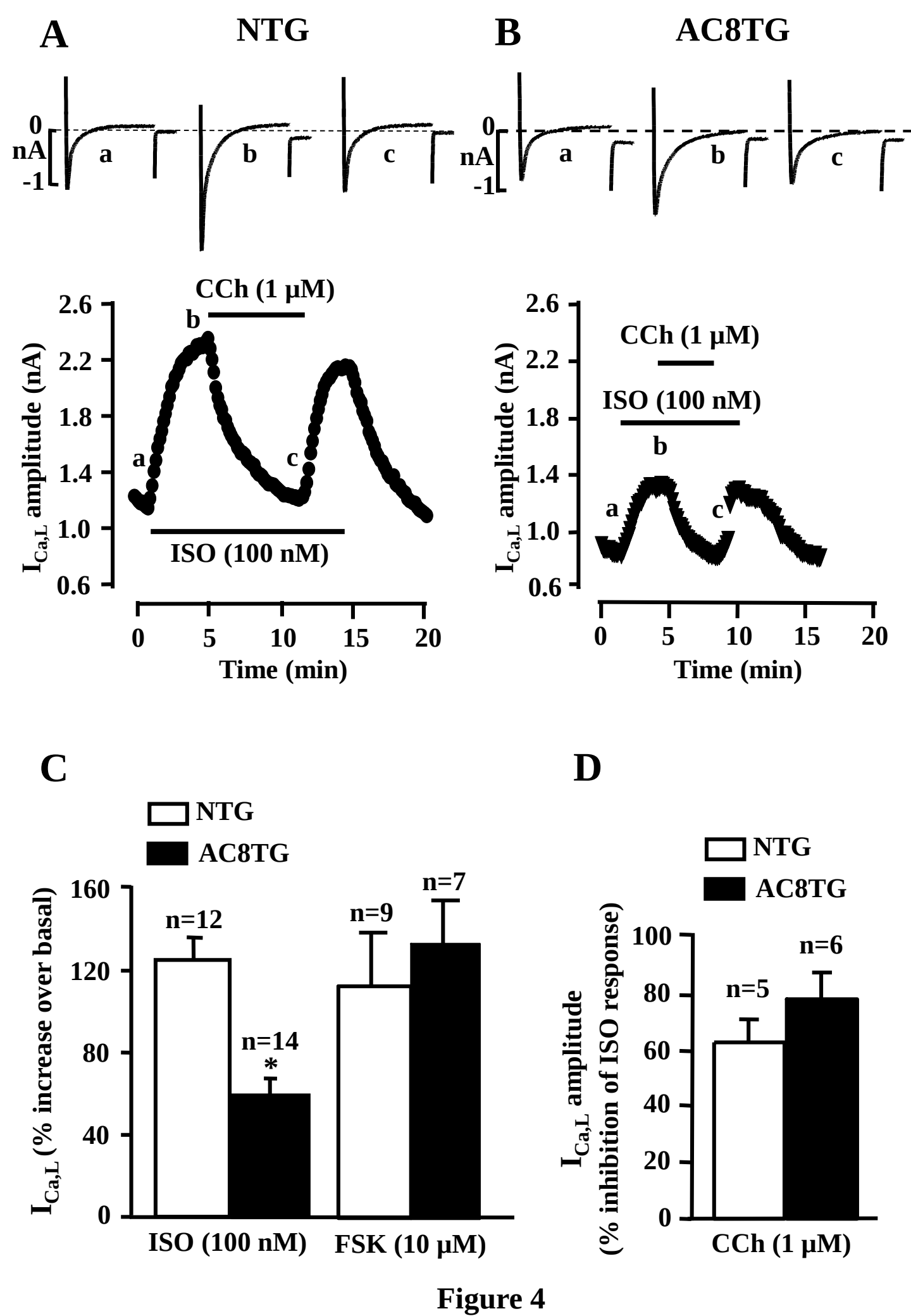
A
NTG
B
AC8TG
0
nA
-1
a
b
c
CCh (1 μM)
ISO (100 nM)
$I_{Ca,L}$ amplitude (nA)
2.6
2.2
1.8
1.4
1.0
0.6
0
5
10
15
20
Time (min)
C
D
NTG
AC8TG
$I_{Ca,L}$ (% increase over basal)
160
120
80
40
0
n=12
n=14
*
n=9
n=7
ISO (100 nM)
FSK (10 μM)
$I_{Ca,L}$ amplitude (% inhibition of ISO response)
100
80
60
40
20
n=5
n=6
CCh (1 μM)

Figure 4

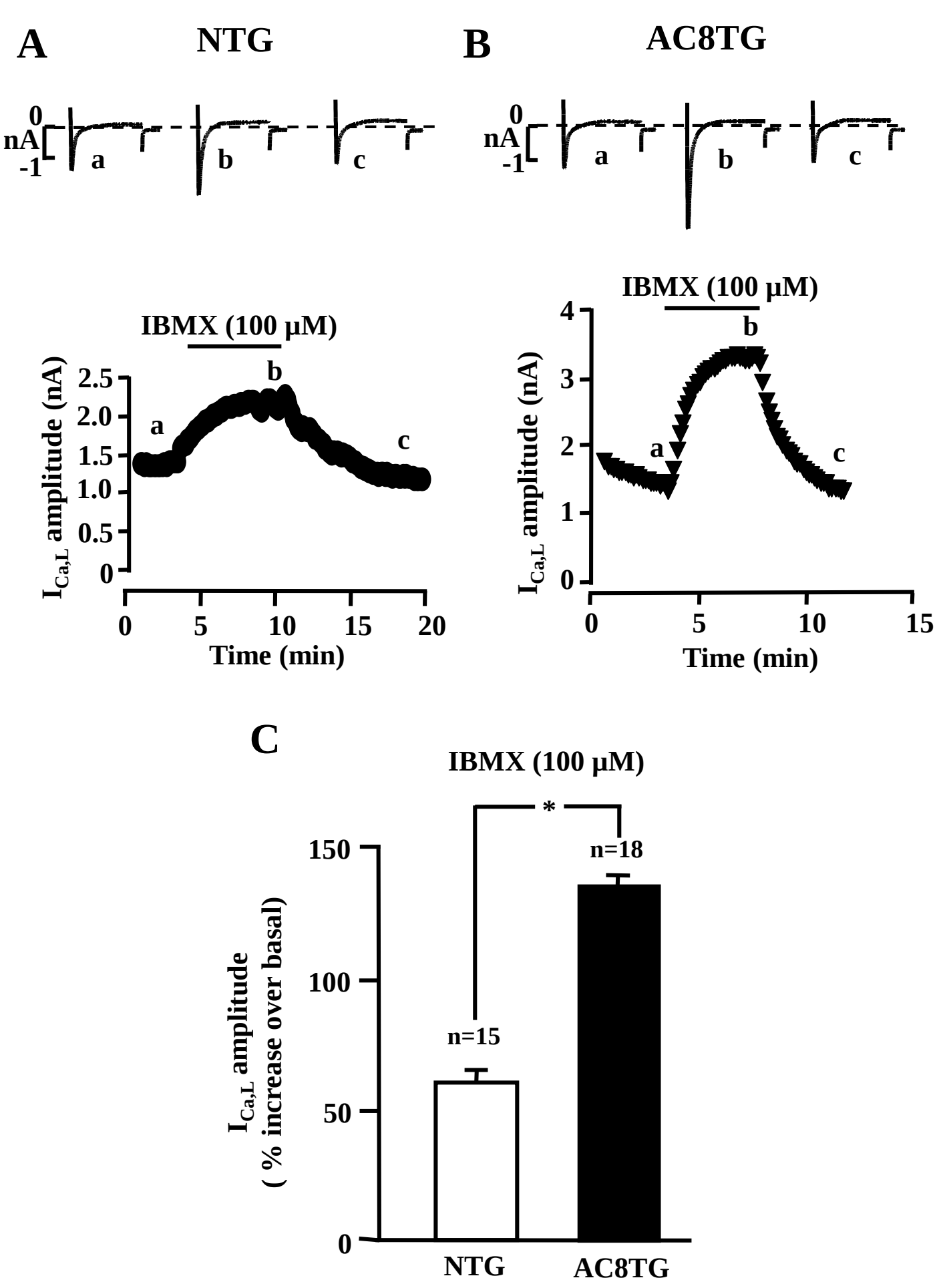
A
NTG
B
AC8TG
0
nA
-1
a
b
c
IBMX (100 μM)
$I_{Ca,L}$ amplitude (nA)
Time (min)
C
IBMX (100 μM)
*
n=18
n=15
$I_{Ca,L}$ amplitude
(% increase over basal)
NTG
AC8TG

Figure 5

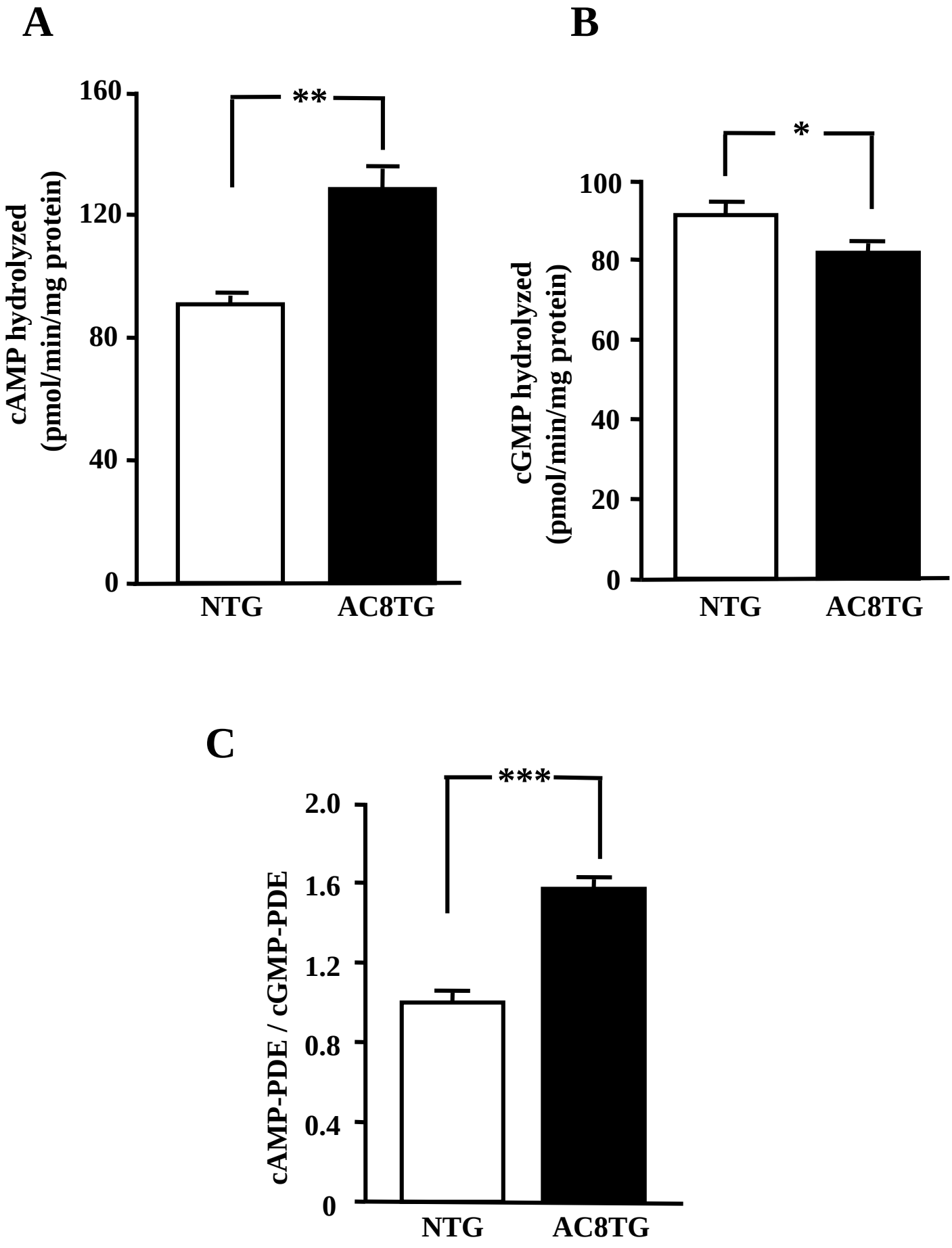
A
160
120
80
40
0
cAMP hydrolyzed
(pmol/min/mg protein)
**
NTG
AC8TG
B
100
80
60
40
20
0
cGMP hydrolyzed
(pmol/min/mg protein)
*
NTG
AC8TG
C
2.0
1.6
1.2
0.8
0.4
0
cAMP-PDE / cGMP-PDE
***
NTG
AC8TG

Figure 6

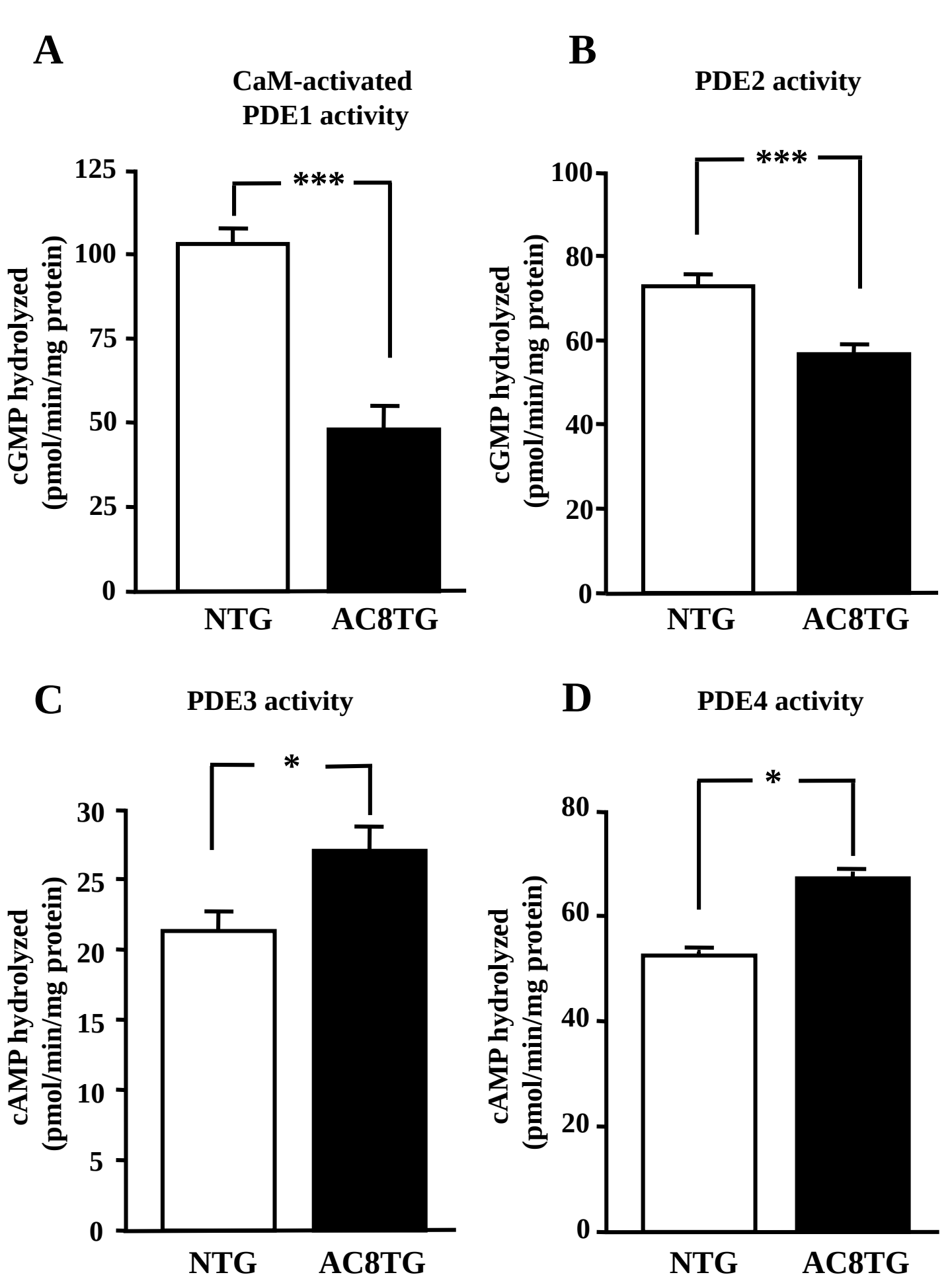
A
CaM-activated
PDE1 activity
cGMP hydrolyzed
(pmol/min/mg protein)
125
100
75
50
25
0
***
NTG
AC8TG
B
PDE2 activity
cGMP hydrolyzed
(pmol/min/mg protein)
100
80
60
40
20
0
***
NTG
AC8TG
C
PDE3 activity
cAMP hydrolyzed
(pmol/min/mg protein)
30
25
20
15
10
5
0
*
NTG
AC8TG
D
PDE4 activity
cAMP hydrolyzed
(pmol/min/mg protein)
80
60
40
20
0
*
NTG
AC8TG

Figure 7